

Figure 8.11 Close-Up of MVDL Estimated Dispersion Curve

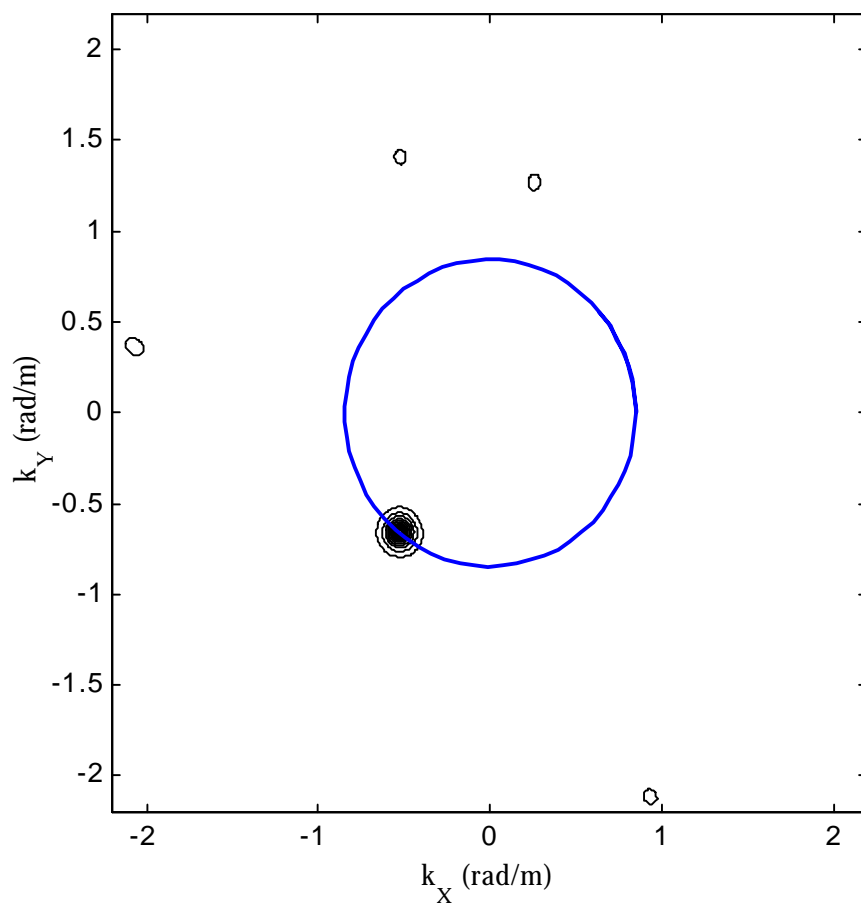


Figure 8.12 Passive Source MUSIC f- \mathbf{k} Power Spectrum Estimate at 24.5 Hz. The MUSIC method estimated a phase velocity of 181.86 m/sec. The noise subspace dimension equals 15 in this case.

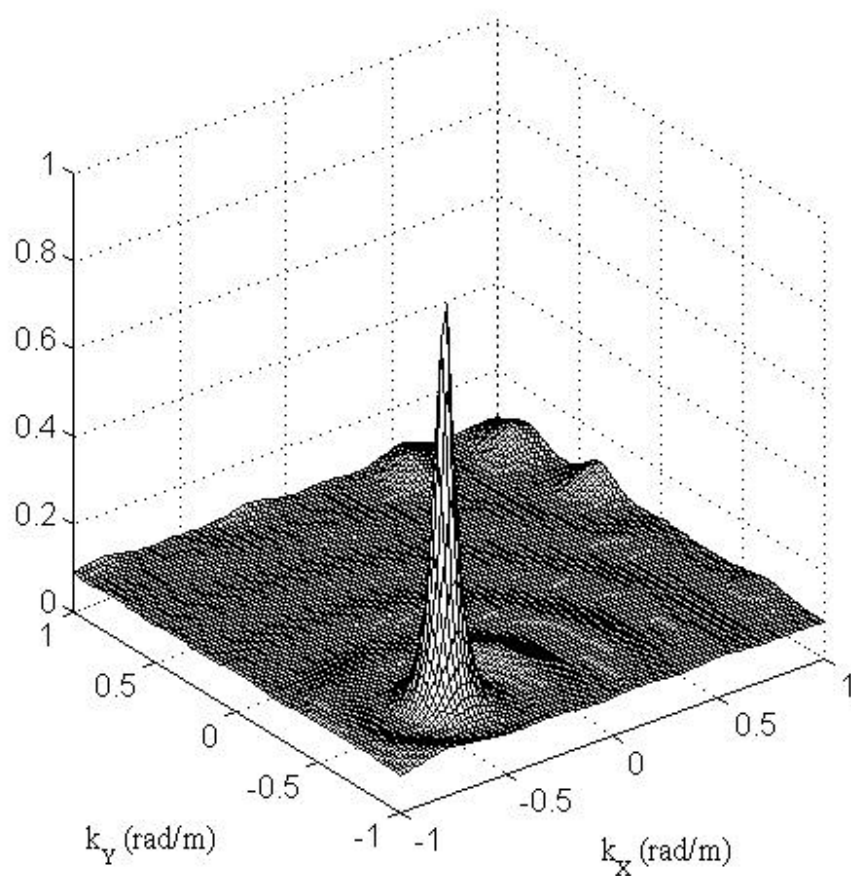


Figure 8.13 Mesh Plot of MUSIC f- \mathbf{k} Estimate at 24.5 Hz with a Noise Subspace Dimension Equal to Fifteen

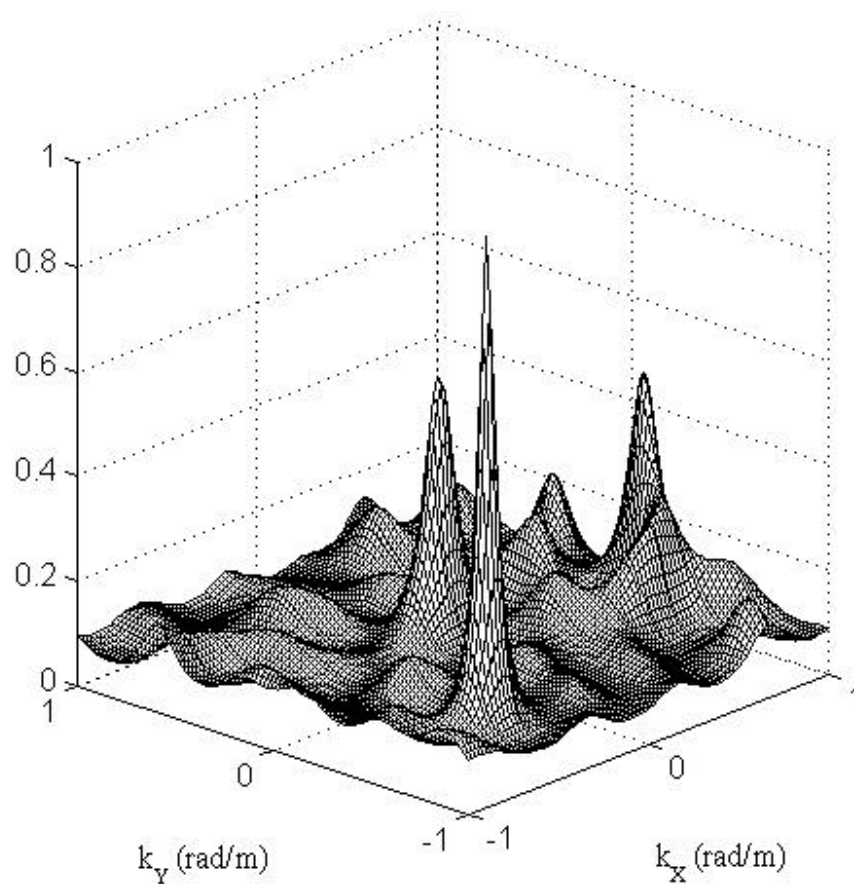


Figure 8.14 Passive Source MUSIC f-**k** Power Spectrum Estimate at 24.5 Hz with a Noise Subspace Dimension Equal to Eight

8.4.4 Comparison of Estimators

MUSIC exhibits the best results for the I85 site presented, exhibiting narrower signal related peaks and less scatter over a wide range of frequencies. Therefore, utilizing only the noise subspace yielded better wavenumber estimates than using the entire inverse spatospectral correlation matrix. The FDBF was shown to be a viable estimator of passive surface wave phase velocities. Linear prediction did not yield acceptable phase velocity estimates, which is not completely unexpected due to the limitations discussed in Chapter 4.

8.4.5 Multiple Signals

Multiple signal arrival or multiple modes may affect the phase velocity estimate, especially when the signal spacing in the wavenumber domain becomes close. Figure 8.17 shows an example FDBF power spectrum estimate containing multiple signals. The power

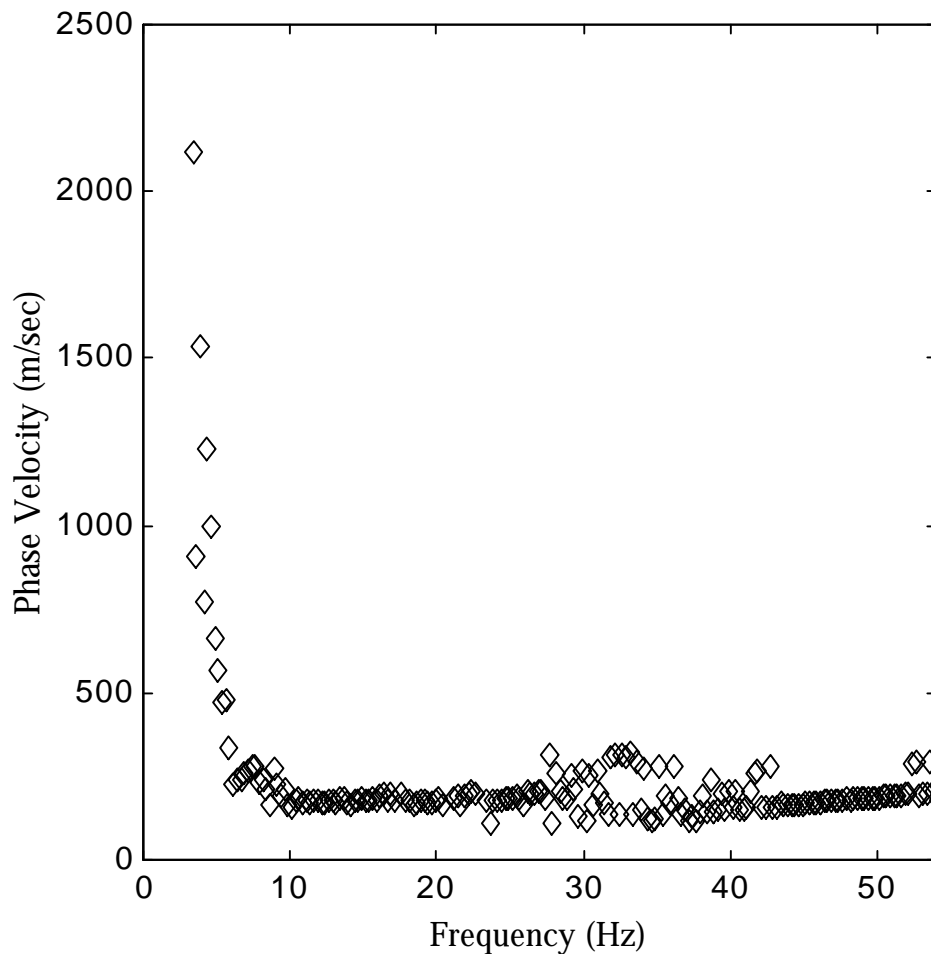


Figure 8.15 MUSIC Dispersion Curve Estimate

estimate spreads out along the circle related to the site-specific natural wavenumber. Sidelobes become important in multiple signal wavefields, since the sidelobes may reinforce to yield spurious peaks.

8.4.6 Direction of Arrivals

Spatial stationarity of the source location is an important consideration in passive surface wave analysis. In the active test, the source location is fixed, allowing *a priori* knowledge of propagation direction. In the passive test, the signal may change direction and range as a function of frequency and time. Figure 8.18 shows the vector direction of arrival of the dominant signal as a function of frequency at the I85 site. The direction of arrival is given by the peak wavenumber (k_x , k_y) values. Although the direction changes at different frequencies, the consistent direction for frequencies in particular ranges is excellent. The higher frequency energy, about 15 to 50 Hz, are due to the highway traffic, while the lower frequency energy probably propagates from a different energy source.

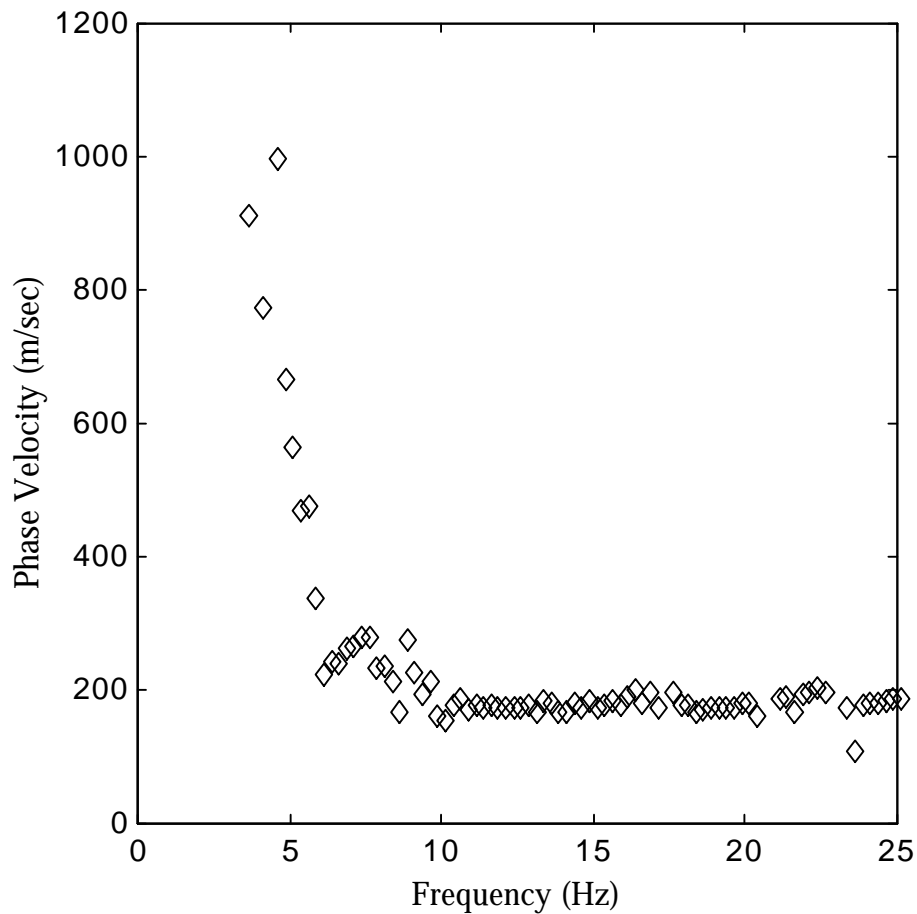


Figure 8.16 Close-Up of MUSIC Estimated Dispersion Curve

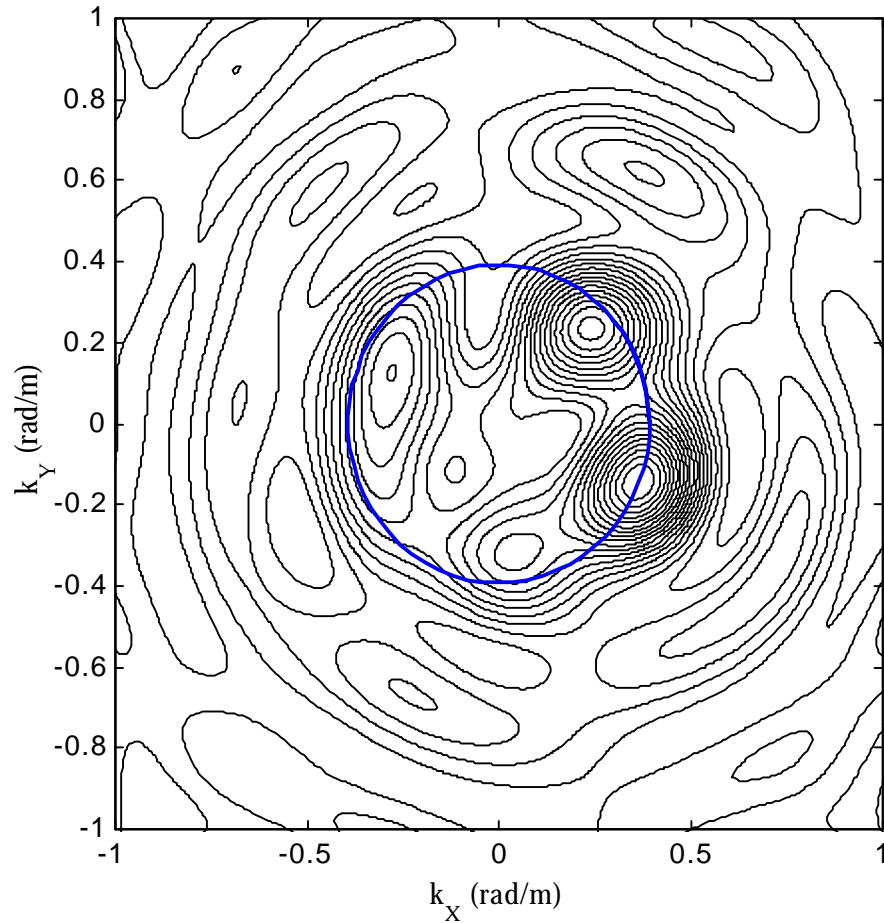


Figure 8.17 Example of Multiple Signals Arriving at a Frequency = 9.875 Hz.

8.5 Material Attenuation Estimation

Two passive surface wave attenuation estimation methods, analogous to the active attenuation estimation methods, are introduced. The least-squares fit of a plane uses the displacement magnitudes measured across the array to determine a minimum wavenumber attenuation estimate. The use of sub-arrays allows estimation of the dominant mode attenuation coefficients. In the least-squares fit of a plane, the noise background is removed using the minimum eigenvalue of the spatio-spectral correlation matrix.

8.5.1 Least-Squares Fit of a Plane

Least-squares fitting a plane to the displacement magnitudes uses the following linear algebra equation

$$A\alpha = b \quad (8.4)$$

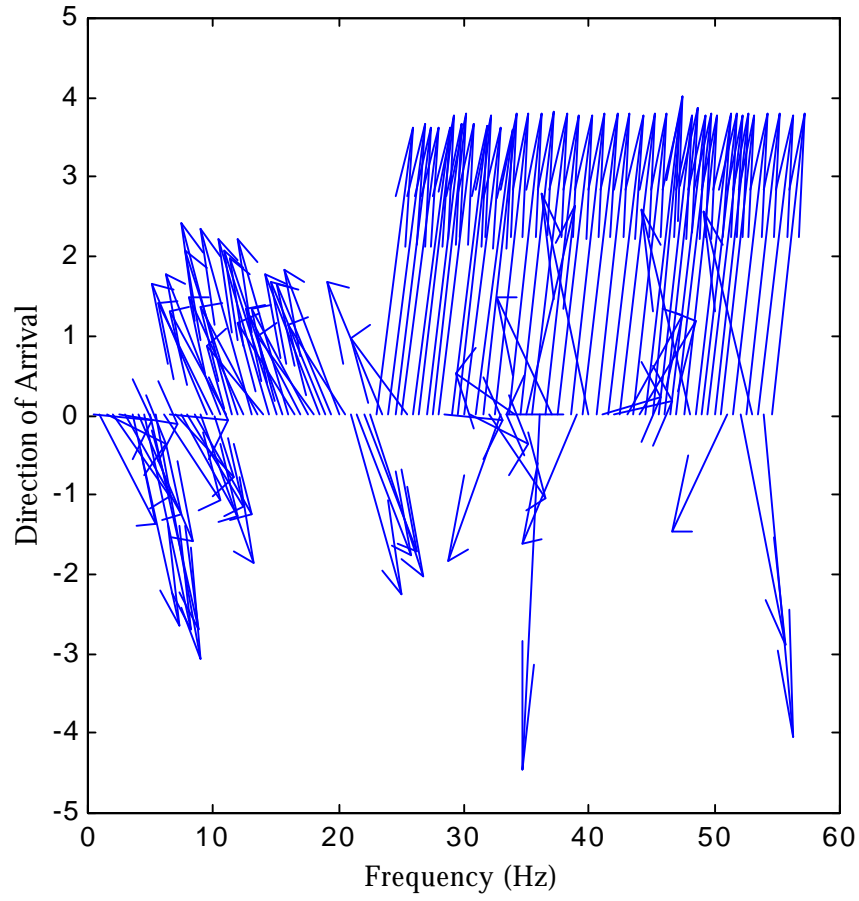


Figure 8.18 Direction of Arrival of Dominant Energy Signal as a Function of Frequency

where the matrix A is the same for all frequencies and equals

$$A = \begin{bmatrix} x_1 & y_1 & 1 \\ x_2 & y_2 & 1 \\ \vdots & \vdots & \vdots \\ x_S & y_S & 1 \end{bmatrix} \quad (8.5)$$

where x and y = the sensor position on the x -axis and y -axis for the sensor given by the subscript, and the column of ones is used to determine the regression intercept. The vector \mathbf{b} = the displacement magnitudes as a function of frequency

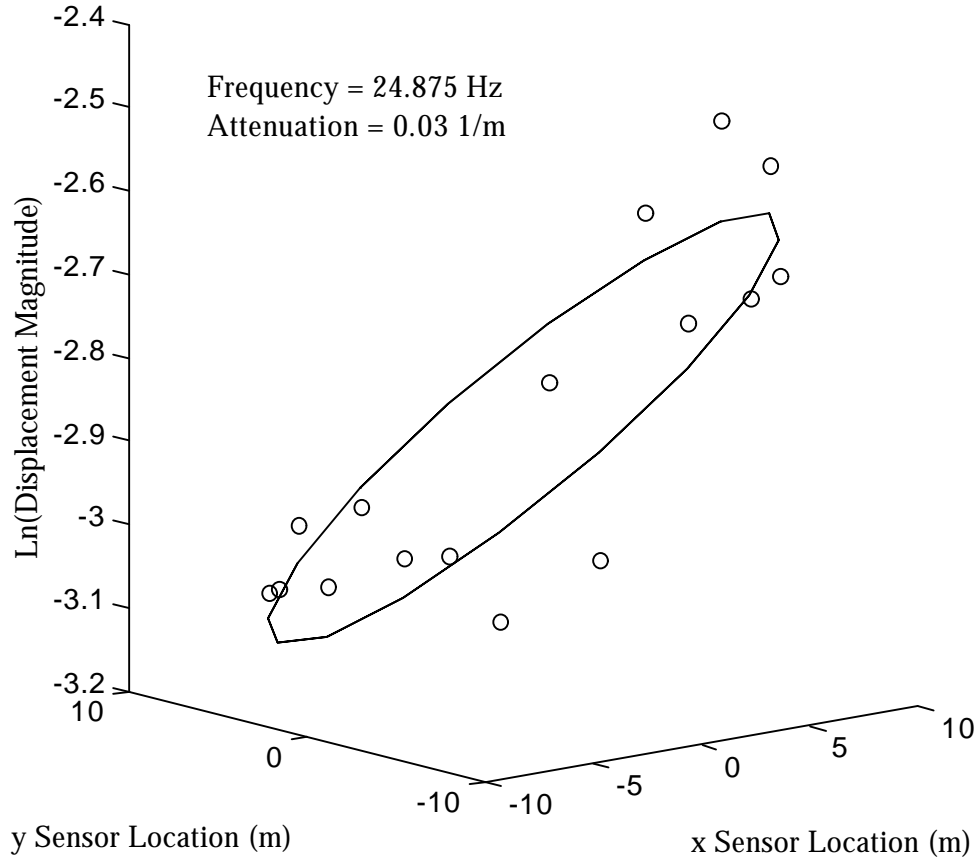


Figure 8.19 Least-Squares Fit of a Plane to Spatial Array Displacement Magnitudes

$$\mathbf{b}(\omega) = \begin{bmatrix} |S_1(\omega)| & |S_2(\omega)| & \cdots & |S_S(\omega)| \end{bmatrix}^T \quad (8.6)$$

where $S(\omega)$ = the displacement magnitude at the subscripted sensor index, for sensors = 1 to S , and the vector α = the regression parameters as a function of frequency

$$\alpha(\omega) = \begin{bmatrix} \alpha_x(\omega) & \alpha_y(\omega) & F(\omega) \end{bmatrix}^T \quad (8.7)$$

where $\alpha_x(\omega)$ and $\alpha_y(\omega)$ equal the attenuation coefficient in the x and y-axis directions for the frequency ω and $F(\omega)$ = the regression intercept.

To solve the least-squares problem, multiply both sides of Equation 8.4 by the Hermitian transpose of the matrix A

$$\mathbf{A}^H \mathbf{A} \boldsymbol{\alpha} = \mathbf{A}^H \mathbf{b} \quad (8.8)$$

and rearrange by taking the inverse of the left-side inner-product $\mathbf{A}^H \mathbf{A}$, yielding

$$\boldsymbol{\alpha} = (\mathbf{A}^H \mathbf{A})^{-1} (\mathbf{A}^H \mathbf{b}) \quad (8.9)$$

where $\boldsymbol{\alpha}$ = the objective function of the minimization of the error as a function of frequency. The background noise power is removed by subtracting the square root of the smallest eigenvalue of the spatio-spectral correlation matrix from the displacement magnitude estimates, since from eigenanalysis, the minimum eigenvalue equals the noise power.

Figure 8.19 shows the attenuation coefficient estimated from fitting a plane to the noise corrected displacement magnitudes at a frequency = 24.875 Hz. Figure 8.20 shows

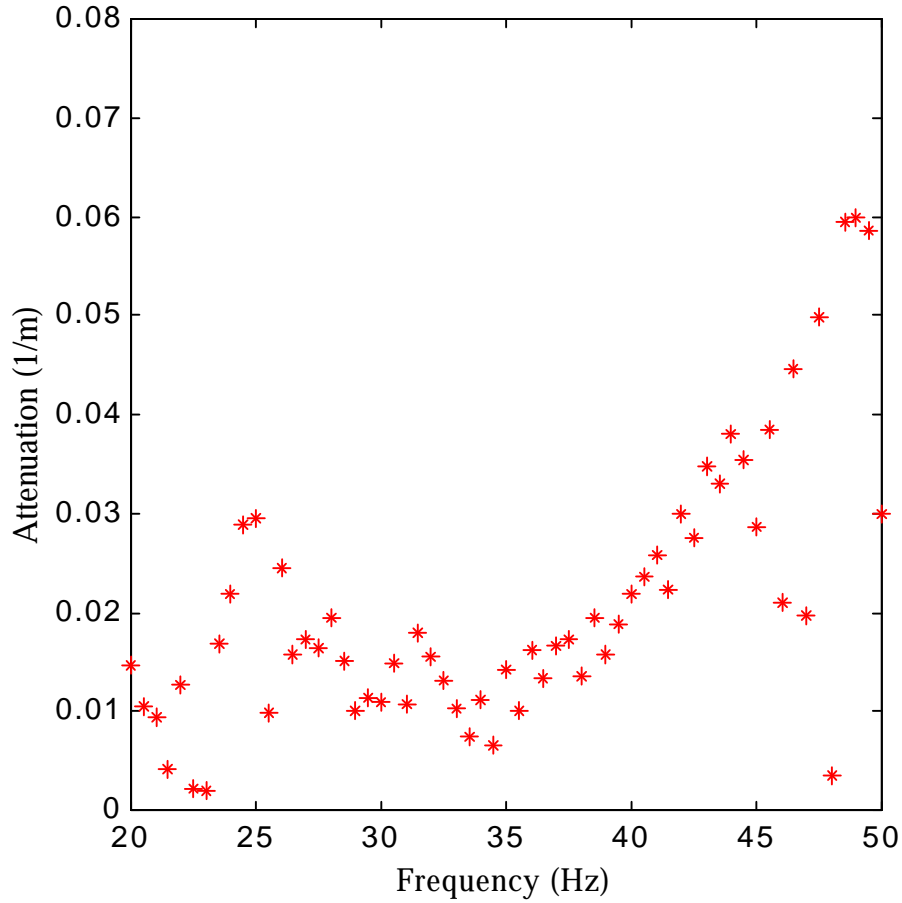


Figure 8.20 Attenuation Curve from Least-Squares Fitting a Plane to Measured Magnitudes

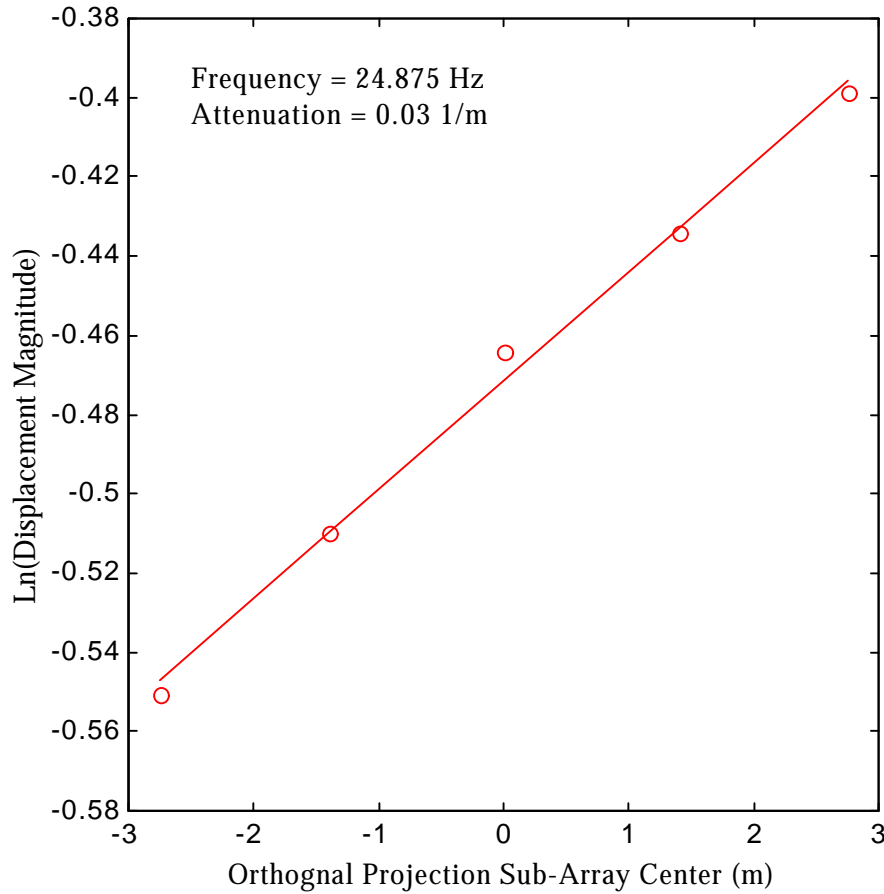


Figure 8.21 Orthogonal Sub-Array Projection Material Attenuation Estimation Method

the attenuation curve estimated from fitting a plane to the displacement magnitudes at all frequencies. The attenuation coefficient estimates follow expectations. To estimate attenuation below 20 Hz, larger array dimensions must be used.

8.5.2 Sub-Array Orthogonal Projection Method

An additional method, which offers the greatest future potential with the deployment of more sensors, larger arrays, or more efficiently designed sub-array geometries, is the orthogonal projection sub-array method. The sub-array method is analogous to the active attenuation sub-array method, and the orthogonal projection allows the sub-arrays to be aligned along the direction of propagation. The optimization problem uses Equation 8.4, except only a single attenuation parameter for each frequency is sought.

After determining the direction of propagation, the sensors are projected onto the axis of propagation for a given frequency with the following equation

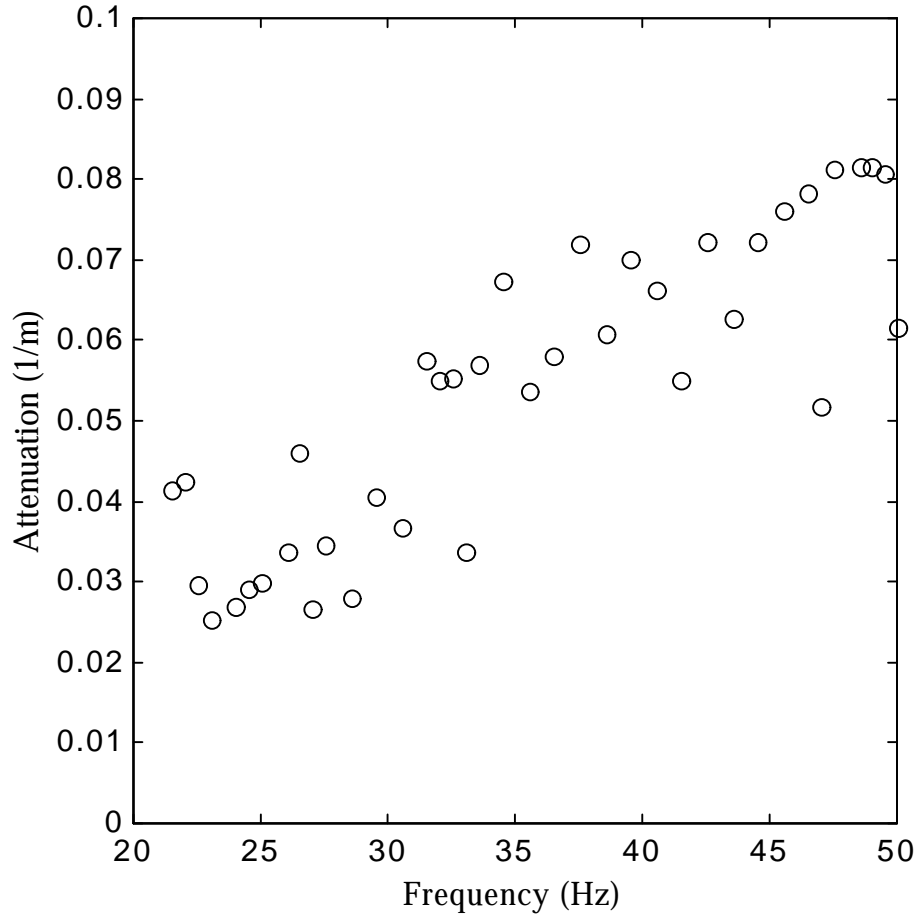


Figure 8.22 Attenuation Curve from Orthogonal Sub-Array Projection Method

$$\mathbf{p}(\mathbf{k}) = \mathbf{k} \frac{\mathbf{k}^T \mathbf{x}}{\mathbf{k}^T \mathbf{k}} \quad (8.10)$$

where

$$\mathbf{p}(\mathbf{k}) = [\mathbf{x}_{1,\text{projected}}(\mathbf{k}) \quad \mathbf{x}_{2,\text{projected}}(\mathbf{k}) \quad \cdots \quad \mathbf{x}_{3,\text{projected}}(\mathbf{k})]^T \quad (8.11)$$

equals the sensor locations projected onto the axis of propagation, and

$$\mathbf{x} = \begin{bmatrix} x_1 & y_1 \\ x_2 & y_2 \\ \vdots & \vdots \\ x_S & y_S \end{bmatrix} \quad (8.12)$$

equal the x and y-axis sensor locations for sensors = 1 to S.

The projection problem is equivalent to the problem defined by Equation 8.4. Defining a projection matrix P

$$P(\mathbf{k}) = \frac{\mathbf{k}\mathbf{k}^T}{\mathbf{k}^T\mathbf{k}} \quad (8.13)$$

the projected sensor locations equal

$$\mathbf{p}(\mathbf{k}) = P(\mathbf{k})\mathbf{x} \quad (8.14)$$

See Strang (1993) for more details concerning projection and minimization of error with linear algebra.

After projection of the measurements onto the axis of propagation, the attenuation coefficient is estimated in the same procedure as for the active source sub-array method. Figure 8.21 shows the orthogonal sub-array projection method for frequency = 24.875 Hz, and Figure 8.22 shows the attenuation coefficients for frequencies between 20 and 50 Hz estimated with five sub-arrays of eleven sensors. Removal of ambient seismic noise yielded poor attenuation estimates in the sub-array method, probably due to less ability to properly estimate the small magnitude eigenvalues with the smaller array.

8.5.3 Discussion

Fitting a plane to the displacement magnitudes yielded excellent attenuation estimates, although the procedure does not filter competing signals. The ability to remove ambient noise energy with the smallest eigenvalue estimate allows better attenuation estimates in stationary noise environments. Although the sub-array method did not yield improved estimates in this case, the sub-array method offers the greatest potential for passive multimode attenuation estimates. The sub-array method is able to reduce the effects of competing signals, and when larger dimensions and optimized sub-arrays are deployed, the method should yield better estimates.

8.6 Signal Modeling

Figure 8.23 shows the match of the experimentally measured data projected onto the axis of propagation, i.e. along the direction of the dominant wavenumber, with the estimated attenuation coefficient for frequency = 24.875 Hz. Notice the sinusoidal nature of the spatial disturbance and the nice fit of the estimated wavelength and attenuation.

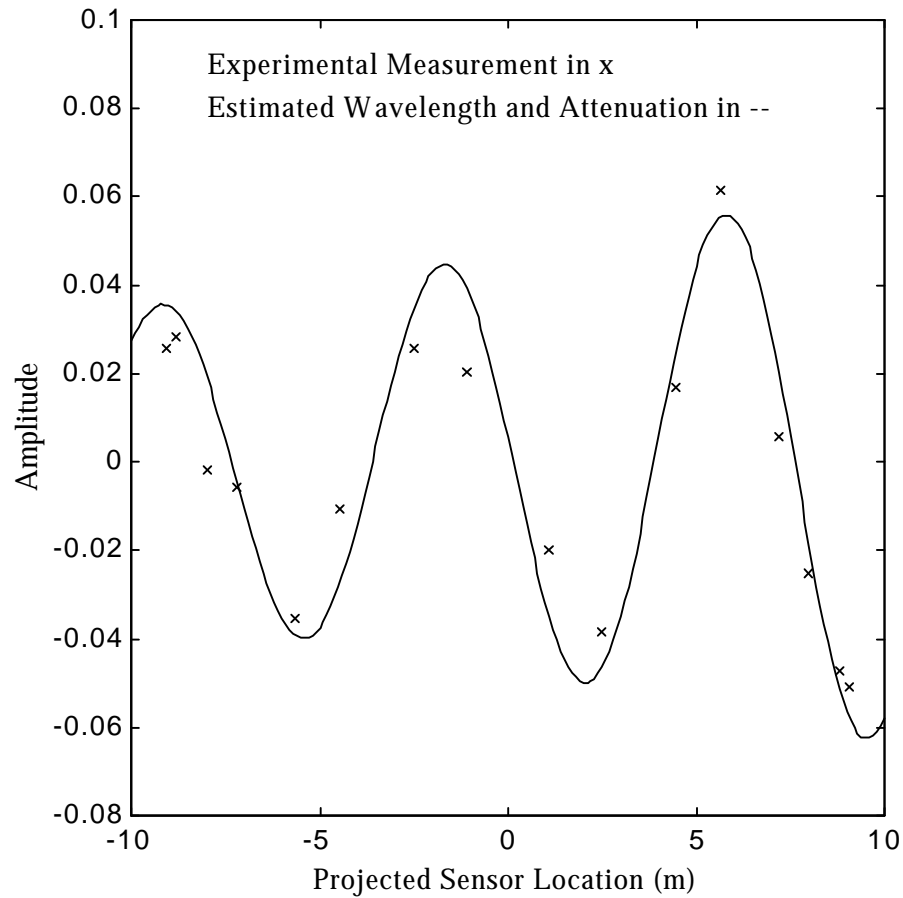


Figure 8.23 Signal Modeling Using Estimated Wavelength and Attenuation for Frequency = 24.875 Hz.

8.7 Summary and Conclusions

The primary advantage of passive surface wave analysis is the plane wave nature of the measurements. As discussed in Chapters 6 and 7, the model incompatibility of traditional active source estimators has caused a tremendous amount of confusion in engineering analysis of seismic surface waves. The passive wave analysis problem mitigates the near-field and model incompatibility problems when measurements are conducted in the far-field.

The MUSIC and FDBF methods yield the best dispersion curve estimates, with MUSIC having narrower signal related peaks. MUSIC, FDBF, and MVDL all yielded similar dispersion curve estimates, but MVDL had more scatter at lower and higher frequencies. The passive dispersion curve estimators appear to isolate several modes, especially at higher frequencies, and larger array dimensions will allow greater resolution at lower frequencies. The linear prediction method did not yield good phase velocity estimates in the passive source problem.

Two passive attenuation coefficient estimators were introduced. The methods are analogous to the active source attenuation estimators discussed in Chapter 7. Least-squares fitting a plane to the noise corrected displacement magnitude yielded excellent results, and the resulting attenuation coefficient estimate corresponds to the smallest wavenumber in the wavefield. Although the orthogonal sub-array projection method did not yield superior results in this case, the sub-array method offers the greatest potential for future passive attenuation coefficient estimation.